dissolved in the start buffer (10 nM monothioglycerol (MTG), 0.25 M sucrose, 25 mM imidazole, pH 7.0) for a chromatofocusing column (1 × 40 cm). This column yields a peak of estrogen sulfurylating activity that is stable for weeks at 0 °C and for months at −20 °C. The chromatofocusing column is eluted with Polybuffer-74 (pH 5.0) diluted 1 to 10 with 2× sucrose–MTG and H_2O to give a final concentration equal to the starting buffer. This gives a pH range for the column of 5.0–7.0. The estrogen sulfotransferase is eluted at pH 6.1, and 1.0-mL aliquots are quick-frozen in liquid nitrogen and stored at −40 °C in 0.25 mM dithiothreitol. Although still a crude enzyme preparation, the peak of estrogen sulfotransferase activity from this chromatofocusing column has separated from the majority of the supernatant proteins and has apparently been freed from the deactivating factors in the tissue supernatant.

(b) Standard Sulfotransferase Assay. The enzyme assay is carried out as published previously.[5,8] Contained in a total volume of 0.2 mL are 0.1 mM PAPS, estrone (E_1) 0.3 μM (60 pmol) in Me_2SO–H_2O (90:10), [6,7-^{3}H]estrone (~1 × 10^6 dpm or 7 pmol), 12 mM magnesium acetate, 0.14 M Tris-HCl buffer, pH 7.8, and 12.7 μg of enzyme preparation. Incubation is carried out for 30 min at 37 °C and the reaction stopped by placing the tubes into boiling water for 4 min. The reaction products may then be extracted into ethyl acetate and the sulfurylated steroids resolved on instant thin-layer chromatography before the radioactivity in the two labels is measured by liquid scintillation counting with absolute activity analysis.[5,8] This assay is also utilized in the kinetic, specificity, and inhibition studies in which case two (10 and 100 times the substrate concentration) concentrations of the compounds (inhibitors) are added to the incubation mixture in 5 mL of Me_2SO–EtOH (90:10). The data are subjected to kinetic analysis, with Lineweaver–Burk plots yielding K_m and V_{max} values. computer analysis (NONLIN program) was employed to corroborate the K_m and V_{max} data derived by hand-drawn plots (Lineweaver–Burk). The inhibition values (apparent K_i) were calculated from fractional inhibition data utilizing the equations described in ref 8. The apparent K_m of porcine endometrial estrogen sulfotransferase for reactions involving estrogen is 10^{-8} M,[16] not unlike that reported for the enzyme from human endometria.[38]

Acknowledgment. This investigation was supported, in part, by a grant from the U.S. Public Health Service (Grant CA 37387) and an institutional grant to the Michigan Cancer Foundation from the United Foundation of Greater Detroit.

(38) Tseng, L.; Mazula, J. In *Proceedings of 8th Brook Lodge Conference on the Problem of Reproductive Physiology*; Kimball, F. A., Ed.; Spectrum Publishing: New York, 1980; p 211.
(39) Goldkamp, A. H.; Hoehn, W. M.; Mikulec, R. A.; Nutting, E. F.; Cook, P. L. *J. Med. Chem.* **1965**, *8*, 409.

Conformational Energy Calculations and Electrostatic Potentials of Dihydrofolate Reductase Ligands: Relevance to Mode of Binding and Species Specificity

P. R. Andrews,* M. Sadek, M. J. Spark, and D. A. Winkler

School of Pharmaceutical Chemistry, Victorian College of Pharmacy Ltd., Parkville, Victoria 3052, Australia.
Received April 15, 1985

Classical potential energy calculations are reported for a series of 11 structurally diverse substrates, products, and inhibitors of dihydrofolate reductase. In almost every case, the calculations reveal a range of potential biologically active conformations accessible to the molecule, and geometry optimization with molecular mechanics and molecular orbital calculations further expands the range of accessible conformations. The energy calculations are supplemented with electrostatic potential energy surfaces for the heterocyclic components of each molecule. These data are used in conjunction with the energy calculations and the crystallographically determined enzyme structures to compare two alternative proposed binding modes of folates known to bind with their pteridine rings inverted relative to that of methotrexate. It is shown that the conformational flexibility of the connecting chain between the benzoyl glutamate and pteridine moieties in the folates actually allows the pteridine ring to shift between these alternative binding modes, a combination of which may offer the best explanation for the observed activity. The electrostatic potentials and conformational energy data are also used in an attempt to account for the species specificity of inhibitors of mammalian, bacterial, and protozoal dihydrofolate reductases. The results show that while these techniques can be used to explain many of the observed results, others require recourse to the observed crystal structures to provide a satisfactory explanation.

Known inhibitors of dihydrofolate reductase (DHFR; 5,6,7,8-tetrahydrofolate NADP$^+$ oxidoreductase, EC 1.5.1.3) vary widely in structure, and many of them display strong species specificity.[1] It is apparent that specificity for binding at the active sites of different DHFRs must eventually depend on the electronic structure and conformational properties of the individual DHFR inhibitors, but the size and conformational flexibility of the molecules is such that these data are generally not available.

In this paper we report complete conformational analyses and electrostatic potentials for a series of compounds representing the major structural classes of DHFR inhibitors (1–8), as well as the substrates and products of the enzyme (9–11). In each case we have used simple classical potential energy calculations, without geometry optimization, to identify all of the biologically accessible conformations. Where necessary, these calculations are supplemented by molecular orbital and molecular mechanics calculations with geometry optimization; molecular orbital calculations have also been used to determine electron distributions and electrostatic potential surfaces. The results indicate that, while all of the ligands share some common electronic properties, virtually all of them can

Table I. Minimum Energy Conformations for the Amide and L-Glutamate Torsion Angles

torsion angle	conformational minima	conformation used for connecting chain calculations
ψ	30° → 140°, −140° → −40°	90°
ϕ	70° → 180°	160°
χ_1	170° → 50°	−70°
χ_2	60° → 60°	180°
ω_1	free rotation	90°
ω_2	free rotation	120°
amide bond	cis/trans	trans

(1) Burchall, J. J. *Ann. N.Y. Acad. Sci.* **1971**, *186*, 143.

0022-2623/86/1829-0698$01.50/0

adopt many different low-energy conformations.

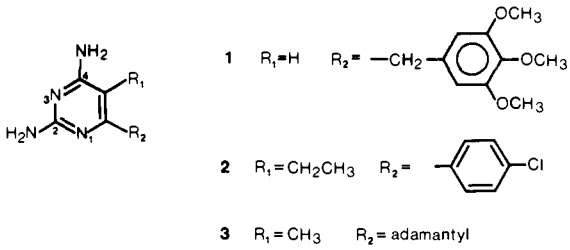

1 R_1=H R_2= —CH_2— 3,4,5-trimethoxyphenyl

2 R_1=CH_2CH_3 R_2= 4-chlorophenyl

3 R_1=CH_3 R_2= adamantyl

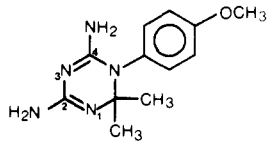

4

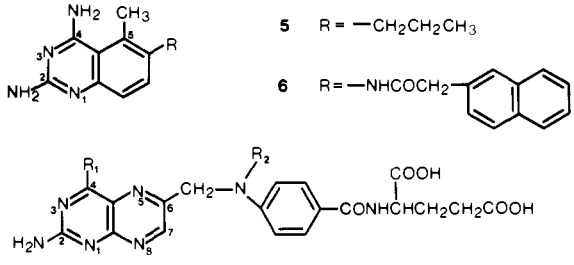

5 R = —$CH_2CH_2CH_3$

6 R = —$NHCOCH_2$— 2-naphthyl

7 R_1 = NH_2 R_2 = CH_3

8 R_1 = NH_2 R_2 = H

9 R_1 = OH R_2 = H

10 7,8-dihydro R_1 = OH R_2 = H

11 5,6,7,8-tetrahydro R_1=OH R_2 = H

The significance of these results is discussed with particular reference to two of the perennial questions relating to DHFR: (1) Why do DHFR substrates bind to the active site with their pteridine rings inverted relative to those of structurally related inhibitors? (2) What is the structural basis for the observed selectivity of small molecule inhibitors for the mammalian, bacterial, or protozoal DHFRs?

Methods

Calculations were performed on Cyber 73 and VAX 11/780 computers at the Royal Melbourne Institute of Technology and La Trobe University, respectively. The program COMOL[2] was used to perform classical potential energy calculations by pairwise summation of the van der Waals interactions between nonbonded atoms, together with electrostatic and torsional potentials. The parameterization used was developed by Giglio[3] on the basis of hydrocarbon and amide structures and has been used to study a number of systems of biological interest.[4-7] The classical calculations were carried out at fixed values of all bond lengths and bond angles, ignoring electrostatic charges. It was shown that these approximations did not alter the qualitative nature of the results, although relaxation of nontorsional degrees of freedom reduced the barriers to rotation between alternative conformations. In each case the variables were considered two at a time, and the potential energy surfaces were calculated with use of rotation intervals of 10°. Torsion angles are defined by clockwise rotations around the appropriate bonds according to the convention of Klyne and Prelog.[8] Conformational potential energy maps were prepared by using a modification of the contouring program KONTOR.[9]

Molecular geometries were obtained from crystal structures[10-15] of related molecules, to which extra groups were added where necessary using geometric parameters from standard compilations.[16] The semiempirical molecular orbital program RPI/MINDO/3[17] was used on selected molecules to optimize geometries and provide quantitative heats of formation. The molecular mechanics program MM2[18] was used to compare the global minimum and bound conformations of folates and folate analogues. Since the MM2 program cannot handle π-systems more complicated than a benzene ring,[19] the pteridine rings in the above structures were preoptimized by using MINDO/3. The carboxylate parameters were obtained by averaging the relevant parameters for the carboxyl group,[20] and the remaining parameters were estimated from those of related molecules. Formal atomic charges calculated by CNDO/2 for minimum-energy conformations (Table I) were used for the MM2 calculations. Because of these extensive approximations, only the van der Waals energies of the minimized geometries were considered in comparing conformations.

In all conformational calculations the molecules were considered with their heterocyclic rings in the neutral form, since these groups exist to a significant extent in the unionized form at physiological pH in all compounds considered other than the dihydrotriazines. It has been reported that methotrexate (7), aminopterin (8), and trimethoprim (1) are protonated when bound to DHFR, while the folates are not,[21-23] but trial calculations showed that protonation (at N_1) did not affect the results of the conformational calculations. The electrostatic calculations (see below) were also carried out on the unionized species, thus identifying the alternative sites (e.g., N_1) for protonation either in solution *or* by interaction with the enzyme. No intermolecular energy calculations were performed. The folates have two possible tautomeric forms, keto or enol. The keto form has been shown to be favored in both so-

(2) Koch, M. H. J. *Acta Crystallogr., Sect. B* **1973**, *29*, 379.
(3) Giglio, E. *Nature (London)* **1969**, *222*, 339.
(4) C'Alagni, M.; Giglio, E.; Pavel, N. V. *Polymer* **1976**, *17*, 257.
(5) Jones, G. P.; Andrews, P. R. *J. Med. Chem.* **1980**, *23*, 444.
(6) Pierri, L.; Pitman, I. H.; Rae, I. D.; Winkler, D. A.; Andrews, P. R. *J. Med. Chem.* **1982**, *25*, 937.
(7) Andrews, P. R.; Mark, L. C. Winkler, D. A.; Jones, G. P. *J. Med. Chem.* **1983**, *26*, 1223.
(8) Klyne, W.; Prelog, V. *Experientia* **1960**, *16*, 521.
(9) Palmer, J. A. B. *Aust. Comp. J.* **1970**, *2*, 27.
(10) Bieri, J. H. *Helv. Chim. Acta* **1977**, *60*, 2303.
(11) Bieri, J. H.; Viscontini, M. *Helv. Chim. Acta* **1977**, *60*, 447.
(12) Koetzle, T. F.; Williams, G. J. B. *J. Am. Chem. Soc.* **1976**, *98*, 2074.
(13) Rogan, P. K.; Williams, G. J. B. *Acta Crystallogr., Sect. B.* **1980**, *36*, 2358.
(14) Schwalbe, C. H.; Hunt, W. E. *Chem. Commun.* **1978**, 188.
(15) Shirrell, C. D.; Williams, D. E. *J. Chem. Soc., Perkin Trans. 2*, **1975**, 40.
(16) Sutton, L. E., Ed. "Tables of Interatomic Distances"; Special Publication No. 11 and 18, The Chemical Society, Burlington House: London, 1958, 1965.
(17) Miller, K. J.; Pycior, J. F.; Moschner, K. *QCPE Bull.* **1981**, *1*, 77.
(18) Allinger, N. L.; Yuh, Y. H. Program MM2, QCPE-395, 1980.
(19) Allinger, N. L. *QCPE Bull.* **1983**, *3*, 32.
(20) Allinger, N. L.; Chang, S. H. M. *Tetrahedron* **1977**, *33*, 1561.
(21) Cocco, L.; Temple, C., Jr.; Montgomery, J. A.; London, R. E.; Blakley, R. L. *Biochem. Biophys. Res. Commun.* **1981**, *100*, 413.
(22) Hood, K.; Roberts, G. C. K. *Biochem. J.* **1978**, *171*, 357.
(23) Subramanian, S.; Kaufman, B. T. *Proc. Natl. Acad. Sci. U.S.A.* **1978**, *75*, 3201.

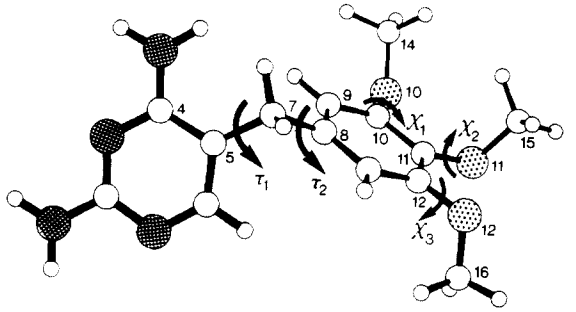

Figure 1. Conformational variables of trimethoprim (1). In this illustration τ_1 ($C_4C_5C_7C_8$), τ_2 ($C_5C_7C_8C_9$), χ_1 ($C_9C_{10}O_{10}C_{14}$), χ_2 ($C_{10}C_{11}O_{11}C_{15}$), and χ_3 ($C_{13}C_{12}O_{12}C_{16}$) are set to −150°, −60°, 60°, 90°, and 30°, respectively.

lution[24] and the crystal state,[25] and this form was therefore assumed throughout this study.

Electron densities were obtained from CNDO/2 calculations, using the program CNDO/INDO.[26] Electrostatic potentials were calculated from the atomic electron densities by utilizing the averaged spherical atomic orbital approximation with complete neglect of differential overlap. Previous applications of this approximation to semiempirical wave functions have been shown to reproduce important features of ab initio calculations.[27,28]

The Victorian College of Pharmacy Ltd. molecular modelling system MORPHEUS was used to perform molecular comparisons, superimpositions, docking of inhibitors into the active site of DHFR *Lactobacillus casei* and DHFR *Escherichia coli*, and measurements of interatomic distances. MORPHEUS is based upon a molecular modelling program developed by P. Pauling, D. Richardson, and M. Lee at University College, London, with additional programs in the package being written by C. Lowther, G. Quint, D. Richardson, and D. Winkler at the Victorian College of Pharmacy. Hard-copy plots of molecular structure were generated using PLUTO, written by S. Motherwell and modified by G. Jones and D. Winkler. The coordinates for DHFR enzymes were obtained from the Brookhaven Protein Data Bank.

Results and Discussion

Conformational Calculations. Although limited conformational calculations have already been performed for some of the small molecule DHFR inhibitors considered here, we nevertheless thought it useful to include representatives of all major classes of DHFR inhibitors in the present calculations. By including all variable torsion angles for each of the substrates and inhibitors, these calculations serve partly to fill in some of the gaps in the existing data and partly to provide an internally consistent set of conformational properties for comparative purposes. Because of the large number of variables considered, the data are presented below in summary form.

The molecular conformation of trimethoprim (1) is determined by two principal torsion angles, τ_1 and τ_2, and the three additional angles χ_1, χ_2, and χ_3, which define the positions of the methoxy groups (Figure 1). Preliminary

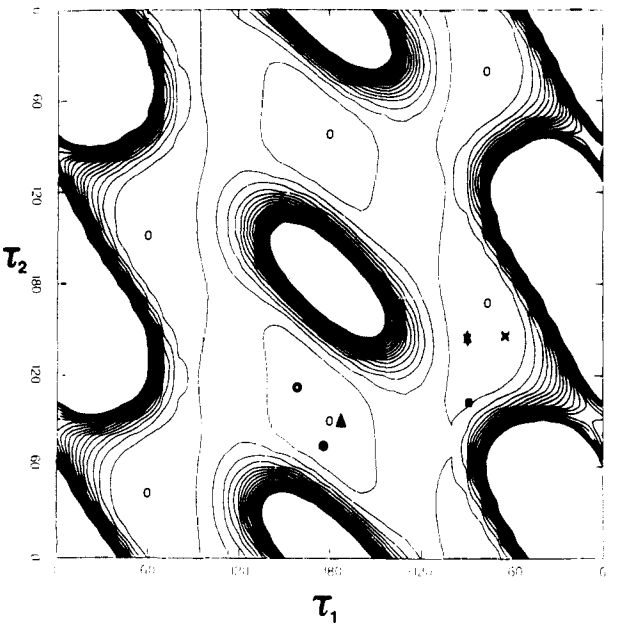

Figure 2. Contour map showing the relative energies of conformations defined by rotations τ_1 and τ_2 in 1. The contour interval is 2.5 kcal/mol, and the first 20 contour lines are shown. The values of the other torsion angles are fixed at $\chi_1 = -80°$, $\chi_2 = 90°$, $\chi_3 = 80°$. The six minimum-energy regions (labeled 0) are degenerate global minima. Observed crystal conformations of TMP and a related compound are as follows: (*) free TMP (ref 12), (x) free *m*-desmethoxy-TMP (ref 31), (○) TMP hydrobromide (ref 32), (▲) TMP–sulphamethoxazole complex (ref 33), (■) chicken DHFR–NADPH–TMP (ref 34), (●) *E. coli* DHFR–TMP (ref 34).

calculations showed that the potential energy surface for rotation of τ_1 and τ_2 is independent of the values chosen for χ_1, χ_2, and χ_3. The two sets of variables were therefore considered separately.

The conformational preferences of the methoxy groups of 1 were determined by calculating potential energy surfaces for χ_1 vs. χ_3 at various fixed values of χ_2. The lowest energy conformations are those for which $\chi_2 = 90°$ or −90°, with χ_1 and χ_3 in the range of 0° ± 90°. Hence, although the 2-methoxy group is restricted to an out-of-plane conformation, the 1- and 3-methoxy groups can adopt either planar or nonplanar conformations. These data are qualitatively consistent[29] with those obtained from ab initio (STO-3G) calculations on *o*-dimethoxybenzene, which favor nonplanar conformations by ca. 1 kcal/mol, and ^{13}C NMR studies of 1,2,3-trimethoxybenzene, in which only the 2-methoxy group is out of plane. Rotation of τ_1 and τ_2 produces the potential energy surface illustrated in Figure 2. There are six individual minima separated by barriers of less than 5 kcal/mol. Symmetry considerations indicate that only three of these (those with different τ_1 values) are distinct conformations, and two of them ($\tau_1 = 60°$ and $\tau_1 = -60°$) are mirror-image conformations. This surface is essentially identical with that obtained previously using similar techniques.[12,30] It is clear that the conformational space accessible to 1 is extremely large, in agreement with the range of conformations observed experimentally for free,[12,31] complexed,[32,33] and

(24) Blakley, R. L. "The Biochemistry of Folic Acid and Related Pteridines" (Frontiers of Biology, Vol. 13); Wiley-Interscience: New York, 1969.
(25) Mastropaolo, D.; Camerman, A.; Camerman, N. *Science (Washington, D.C.)* **1980**, *210*, 334.
(26) Dobosh, P. A. *Quantum Chem. Program Exchange* **1968**, 141.
(27) Giessner-Prettre, C.; Pullman, A. *Theor. Chim. Acta* **1972**, *25*, 83.
(28) Andrews, P. R.; Defina, J. A. *Int. J. Quantum Chem., Quantum Biol. Symp.* **1980**, *7*, 297.
(29) Anderson, G. M., III; Kollman, P. A.; Domelsmith, L. N.; Houk, K. N. *J. Am. Chem. Soc.* **1979**, *101*, 2344. Makriyannis, A.; Fesik, S. *J. Am. Chem. Soc.* **1982**, *104*, 6462.
(30) Hopfinger, A. J. *J. Med. Chem.* **1981**, *24*, 818.
(31) Koetzle, T. F.; Williams, G. J. B. *Acta Crystallogr., Sect. B* **1978**, *B34*, 323.
(32) Phillips, T.; Bryan, R. F. *Acta Crystallogr., Sect. A* **1969**, *A25*, S200.

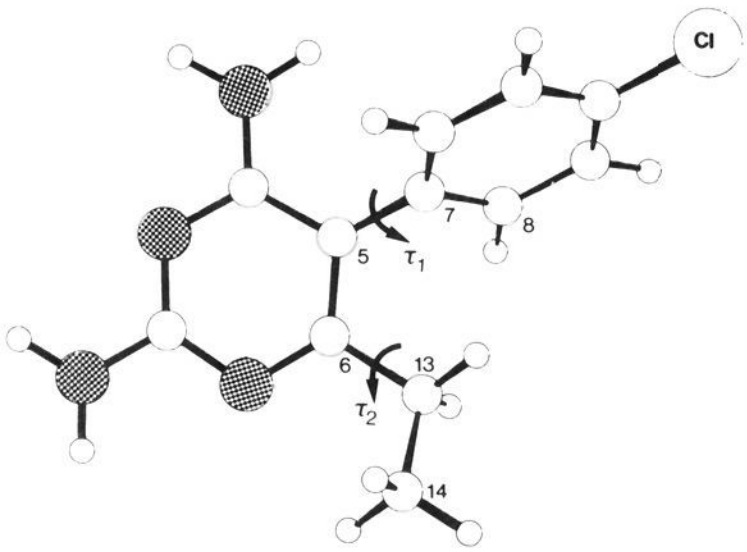

Figure 3. Conformational variables in **2**. The torsion angles are fixed at τ_1 ($C_6C_5C_7C_8$) = 60° and τ_2 ($C_5C_6C_{13}C_{14}$) = 150°.

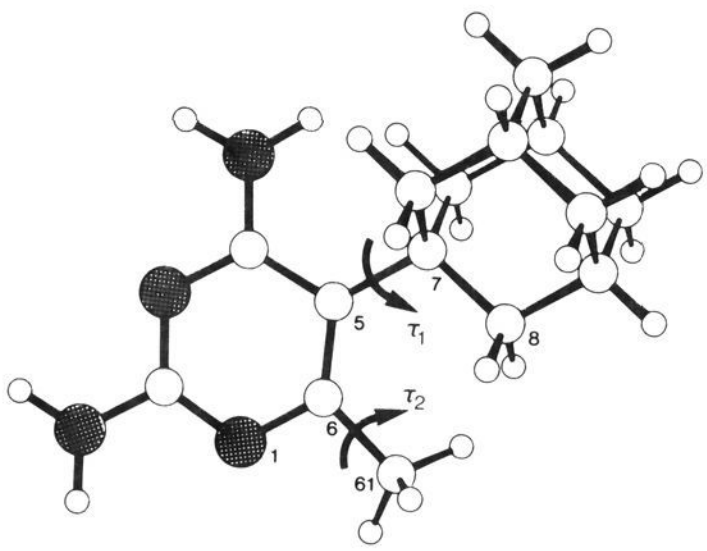

Figure 4. Conformational variables τ_1 ($C_6C_5C_7C_8$) and τ_2 (N_1-$C_6C_{61}H$) of **3**. In this illustration τ_1 = 0° and τ_2 = 80°.

enzyme-bound[34] trimethoprim (Figure 2).

Rotation of the two significant torsion angles (Figure 3) in pyrimethamine (**2**) leads to two broad conformational regions with τ^1 = 90° ± 30° or −90° ± 30° (degenerate conformations) and τ_2 = 180° ± 100°. The observed conformation in the crystal[32] (τ_1 = 67°) is consistent with the calculations.

The potential energy calculations for rotation about τ_1 and τ_2 in 2,4-diamino-5-(1-adamantyl)-6-methylpyrimidine (**3**, Figure 4) lead to nine degenerate conformations with τ_1 or τ_2 = 0°, 120°, or −120°. Each of these regions is relatively small (±10°) due to steric interaction between the adamantyl substituent and adjacent groups. The observed crystal structure[35] falls within these limits (τ_1 = −7.5°), although the diaminopyrimidine ring is substantially distorted from planarity in the crystal. This finding is confirmed by CNDO/2 calculations.[36] The crystal structure of **3** bound to chicken liver dihydrofolate reductase has also been determined but not at sufficient resolution to define the bound conformation.[34]

The dihydrotriazine ring in 2,4-diamino-6,6-dimethyl-5-(*p*-methoxyphenyl)-5,6-dihydrotriazine (**4**) can adopt two mirror-image conformations, with C_6 either above (conformation A) or below (conformation B) the plane of the ring (viewed as in Figure 5). Conformation B was used in the conformational analyses because it is the conformation given in the published crystal structure of cycloguanil,[14] but both stereoconformers are equally accessible.

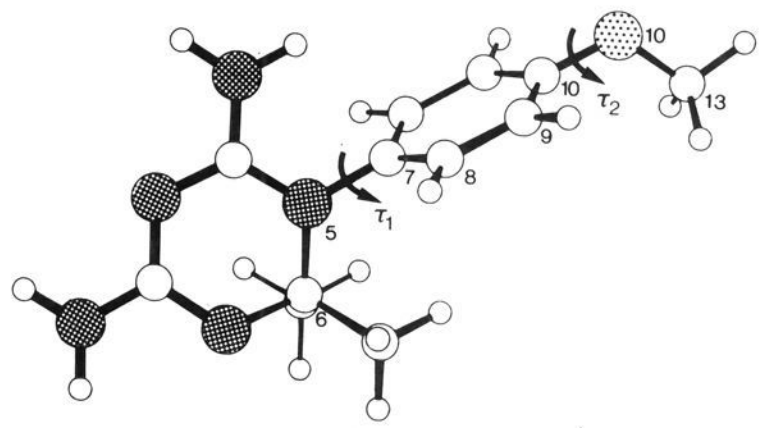

Figure 5. Conformational variables in **4**; in this illustration τ_1 ($C_6N_5C_7C_8$) = −90° and τ_2 ($C_9C_{10}O_{10}C_{13}$) = 90°.

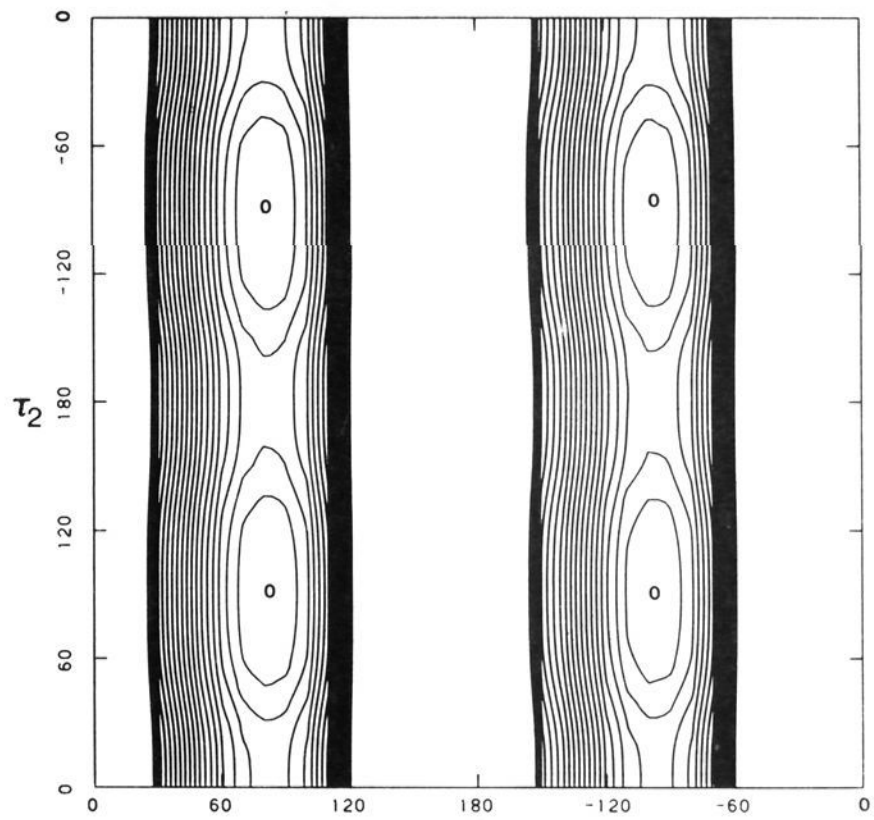

Figure 6. Contour map describing the relative energies for rotations τ_1 and τ_2 of **4**. The first twenty 2.5 kcal/mol contour lines are shown. Energies of minima are given relative to their global minimum.

The two major degrees of conformational freedom in **4** are shown in Figure 5. Rotation of these two torsion angles gives the potential energy surface illustrated in Figure 6. There are four minima, which correspond to two degenerate conformations of **4** with τ_1 = 80° ± 20° or −100° ± 20°, and τ_2 = 90° ± 60° or −90° ± 60°. The experimentally observed conformations of phenyldihydrotriazines[14,37] are within these low-energy regions.

Conformational analyses of phenyldihydrotriazine have also been performed by Ghose and Crippen[38] and Hopfinger.[39] The results obtained by the former authors are in good agreement with ours, but Hopfinger obtained four minima [τ_1 = 30° (≡ −150°), 90° (≡ −90°)], of which two (τ_1 = 30, −150°) are high-energy conformations according to our calculations. MINDO/3 calculations with full geometry optimization were therefore performed on the two distinct conformations (τ_1 = 30° or 90°) of **4** to resolve this difference. These calculations showed that steric interactions between the phenyl ring and the adjacent amine in the conformation with τ_1 = 30° force the amine group

(33) Guiseppeti, C.; Todine, C. *Farmaco Ed. Sci.* **1980**, *35*, 138.
(34) Matthews, D. A.; Bolin, J. T.; Burrdige, J. M.; Filman, D. J.; Volz, K. W.; Kraut, J. *J. Biol. Chem.* **1985**, *260*, 392.
(35) Cody, V.; Zakrzewski, S. F. *J. Med. Chem.* **1982**, *25*, 427.
(36) Walsh, W. T.; Cody, V.; Mark, J. E.; Zakrzewski, S. F. *Cancer Biochem. Biophys.* **1983**, *7*, 27.
(37) Volz, K. W.; Matthews, D. A.; Alden, R. A.; Freer, S. T.; Hansch, C.; Kaufman, B. T.; Kraut, J. *J. Biol. Chem.* **1982**, *257*, 2528.
(38) Ghose, A. K.; Crippen, G. M. *J. Med. Chem.* **1984**, *27*, 901.
(39) Hopfinger, A. J. *J. Am. Chem. Soc.* **1980**, *102*, 7196.

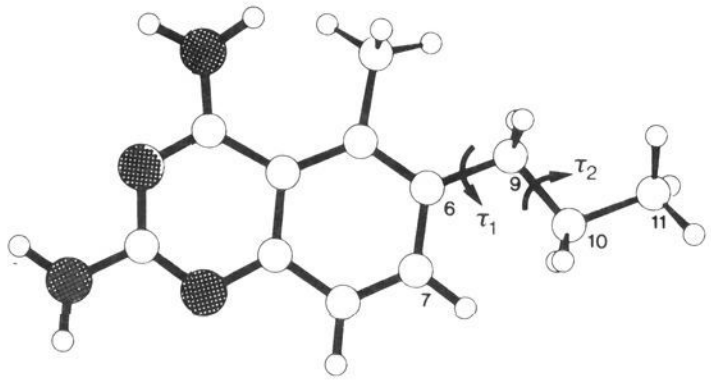

Figure 7. Conformational values in **5**; in this illustration τ_1 ($C_7C_6C_9C_{10}$) = 0° and τ_2 ($C_6C_9C_{10}C_{11}$) = 180°.

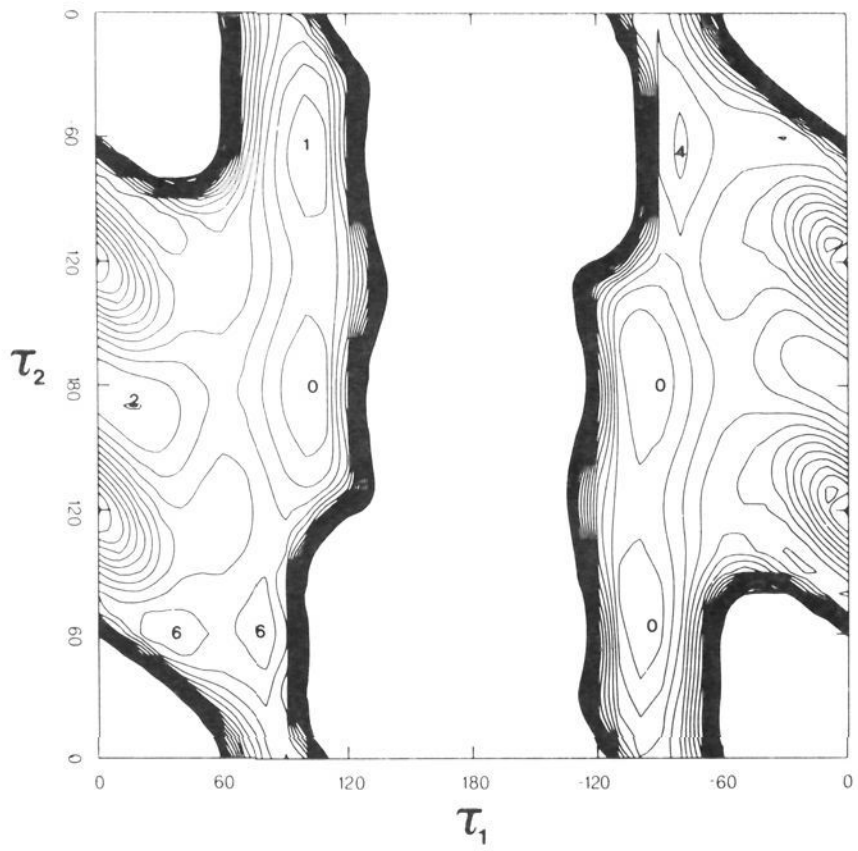

Figure 8. Contour map obtained for the rotations τ_1 and τ_2 in **5**. The contour interval is 2.5 kcal/mol and the first 20 contour lines are shown. Energies of minima are given in kilocalories/mole above the global minimum.

some 15° out of the plane of the conjugated portion of the dihydrotriazine ring, and the resulting energy is 6 kcal/mol higher than that when τ_1 = 90°. We therefore conclude that only the conformational regions with τ_1 near ± 80° and τ_2 near ±90° (degenerate) are geometrically accessible to **4**. Allowing for the other stereoconformer thus gives eight possible conformations for **4**, but these reduce to four distinct conformational regions because of the symmetry of the phenyl ring. These findings are in good agreement with the crystal structures observed for six different phenyldihydrotriazines bound to chicken liver DHFR, each of which has τ_1 near 70°.[34]

2,4-Diamino-5-methyl-6-propylquinazoline (**5**) has two degrees of conformational freedom (Figure 7). The potential energy surface obtained for rotation of these two torsion angles is shown in Figure 8. There are a number of accessible conformations of τ_2, but in each case the side chain is essentially perpendicular to the quinazoline ring (τ_1 = ±90°). There are four conformational variables in 2,4-diamino-5-methyl-6-(2-naphthacetamido)quinazoline (**6**, Figure 9). One of these is the amide bond, which can adopt either a cis or trans conformation. Initially the amide bond was fixed trans, with τ_2 and τ_3 being rotated through 360° for various fixed values of τ_1. There are eight distinct low-energy regions (τ_1 = ±90°, τ_2 = ±90°, τ_3 = ±90°) on the potential energy surface, but the barriers to rotation around τ_2 and τ_3 are very low (<3 kcal/mol). A similar, although more constricted potential energy surface,

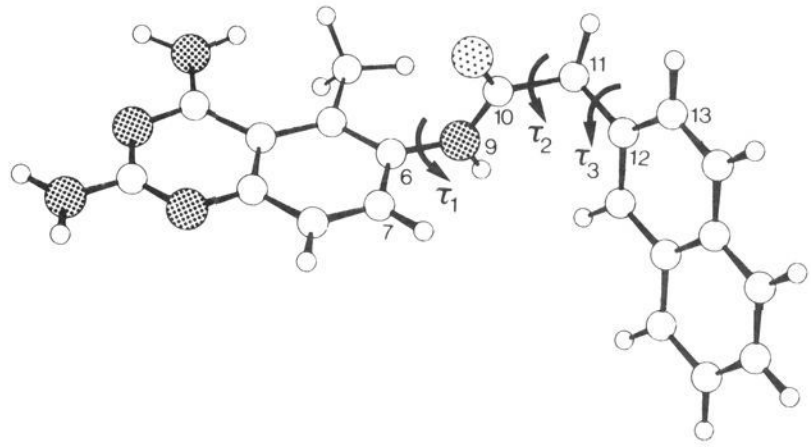

Figure 9. Conformational variables in **6**; in this illustration τ_1 ($C_7C_6N_9C_{10}$) = −90°, τ_2 ($N_9C_{10}C_{11}C_{12}$) = −80°, τ_3 ($C_{10}C_{11}C_{12}C_{13}$) = −70°, and the amide bond ($C_6N_9C_{10}C_{11}$) is in the trans conformation.

is obtained when the amide is in the cis conformation, for which the global minimum is 2 kcal/mol lower than for the trans form.

The five structurally similar folates and folate analogues (**7**–**11**) studied each have nine degrees of rotational freedom (Figure 10), plus an amide bond that can adopt either a cis or trans conformation. The torsion angles can be classified into two independent groups: those in the connecting chain region between the pteridine and benzene rings, and those in the amide/L-glutamate region. Although cis/trans isomerization of the amide bond alters the quantitative nature of the potential energy surfaces obtained for the connecting chain region, the same low-energy conformational regions are obtained in both cases. Since there are no other significant interactions between the two regions, they are considered separately.

The amide/L-glutamate region was analyzed with use of methotrexate (**7**) with the amide bond initially in the trans conformation. The carboxylic acid groups are ionized at physiological pH, so the acid hydrogens were not included in the calculations. Both the carboxylic acid groups are essentially free to rotate with a minimum energy barrier of 2 kcal/mol and preferred positions ω_1 = 90° or −90° and ω_2 = 120° or −60°. The potential energy surface obtained for χ_1 and χ_2 (the torsion angles in the L-glutamate chain) shows minima at χ_1 = 180° and −70° and χ_2 = 60°, 180°, and −60°, with barriers of <5 kcal/mol separating these minima. Rotation of ψ and ϕ, the torsion angles either side of the amide bond, gives a simple potential energy surface with a single broad minimum energy region between ϕ = 60° and −160°. For ψ, there are minima[40] at 90° and −90°, with a barrier of 10 kcal/mol at ψ = 0° and 180°. This part of the potential energy surface is dependent on the position of χ_1 and ω_2. The range of angles accessible to ϕ diminishes when χ_1 is moved from 180° to −70°. Variation of ω_2 affects the barrier height at ϕ = 120° but leaves the position of the minima unaltered. Placing the amide in the cis conformation also leaves the position of the minima unchanged, although the energy barrier between the minima is increased. Summarized in Table I are the minimum-energy values for the

(40) It should be kept in mind that these energy surfaces refer solely to nonbonded van der Waals interactions; i.e., they are based purely on steric factors, without any consideration of electronic effects. Also, these calculations indicate very broad (Table I) minima and a relatively low rotational barrier for the angle ψ. It is commonly understood that the benzamido moiety is nearly planar, but X-ray analyses indicate that this may not always be true, even for simple benzamides. In the crystal structures of bound methotrexate, and out-of-plane (ψ angle) conformation was found at both 2.5- and 1.7-Å resolution (Table II).

Table II. Dihedral Angles and Calculated Energies of Methotrexate in Conformations Bound to Dihydrofolate Reductase from Various Sources

	2.5-Å resolution			1.7-Å resolution		
	L. casei	*E. coli* A	*E. coli* B	*L. casei*	*E. coli* A	*E. coli* B
τ_1	13	0	25	34	28	31
τ_2	63	75	58	57	55	52
τ_3	153	169	180	5	5	16
ψ	97	157	148	149	163	154
θ	185	110	100	123	117	120
χ_1	179	215	180	-68	-79	-80
χ_2	202	127	208	136	-60	-78
ω_1	92	83	107	157	163	161
ω_2	0	327	329	41	145	130
energy *a*	71	27	33	21	20	17
energy *b*	9	4	4	0 (0)	1 (1)	3 (1)

[a] Nonoptimized van der Waals energy (kilocalories/mole). [b] MM2-optimized van der Waals energy (kilocalories/mole). Figures in parentheses are those obtained with use of MINDO/3 optimized pteridine ring geometry.

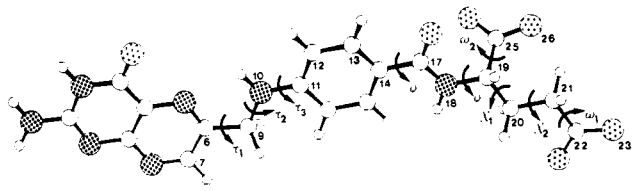

Figure 10. Conformational variables for the folates and folate analogues studied. In this illustration τ_1 ($C_7C_6C_9N_{10}$) = τ_2 ($C_6C_9N_{10}C_{11}$) = τ_3 ($C_9N_{10}C_{11}C_{12}$) = ψ ($C_{13}C_{14}C_{17}N_{18}$) = ϕ ($C_{17}N_{18}C_{19}C_{20}$) = χ_1 ($N_{18}C_{19}C_{20}C_{21}$) = χ_2 ($C_{19}C_{20}C_{21}C_{22}$) = ω_1 ($C_{20}C_{21}C_{22}O_{23}$) ω_2 ($N_{18}C_{19}C_{25}O_{26}$) = 180°.

six torsion angles in the amide/L-glutamate region.

The three torsion angles in the connecting chain region are all dependent upon one another. A three-dimensional approach was therefore used in which τ_2 was incremented in 30° steps from 0° to 360°, while the potential energy surface for rotation of τ_1 and τ_3 was determined. The amide/L-glutamate torsion angles were held in the conformations shown in Table I. This procedure was repeated for each of the folates and folate analogues **7**–**11**.

Four of the potential energy surfaces obtained for the rotation of τ_1 and τ_3 in **7** are illustrated in Figure 11. Potential energy surfaces calculated when τ_2 = -60° or -120° are similar to those for τ_2 = 60° or 120°. The energy barrier to rotation about τ_2 is maximal at 180°; thus the extended conformation is least favored. The minimum-energy conformations of τ_1 and τ_3 are at τ_1 = 90° or -90°, and τ_3 = 90° or -90°, independent of τ_2. Placing the amide in a cis conformation has little effect on the potential energy surfaces for rotation of τ_1 and τ_3, and the positions of the four minima are unaltered. Therefore only the trans amide conformation was considered for the other folates and folate analogues.

Removal of the N_{10}-methyl of **7** to give aminopterin (**8**) reduces the barrier to rotation about τ_1 and τ_2, and to a lesser extent, τ_3. Aminopterin is thus somewhat more flexible than **7**. Further modification of this structure by replacing the 4-amino substituent with a hydroxyl group to give folic acid (**9**) has little effect on the calculated potential energy surfaces. Reduction of the pteridine 7–8 bond to give dihydrofolate (**10**) also has little effect on the calculated potential energy surfaces. Reduction of the pteridine 7–8 bond to give dihydrofolate (**10**) also has little effect on the calculated potential energy surface for rotation of τ_1 and τ_3, although there is some further increase in conformational flexibility when τ_2 falls between 120° and -120°. The calculated low barrier to rotation about τ_2 in **10** is consistent with the results of CNDO/2 calculations on two alternative conformations of a related model structure.[41]

Further reduction of the 5–6 bond of **10** to give tetrahydrofolate (**11**) causes loss of planarity of the pyrazine portion of the pteridine ring, and thus substantial changes in the potential energy surface for rotation around τ_1, for which minima now occur at τ_1 = 90°, 160° or -60°.

There are very few experimental determinations of the conformations of folates and folate analogues, with folic acid being the only one for which a crystal structure is available in the free form.[25] In this structure **9** is in an extended conformation with τ_2 = 180°, and this relatively high energy conformation is apparently stabilized by hydrogen-bond formation with water and intermolecular stacking of the pteridine and phenyl rings. In contrast, methotrexate, which differs from folic acid by substitution of a hydroxy group for the amino group at C4 and replacement of the hydrogen at N_{10} with a methyl group, binds to DHFR in a folded conformation, with $\tau_2 \simeq$ 50–60°.

The crystal structures of methotrexate bound to DHFR *L. casei* and to two conformations of DHFR *E. coli* have been determined.[42,43] In the early stages of our work[44] on this enzyme, these data were only available at 2.5-Å resolution, and energy calculations based on them suggested that the bound conformations of methotrexate were extremely high in energy (Table II). As noted in our preliminary publication,[44] this could have been due to the poor resolution of the available crystal data or the absence of full geometry optimization in our molecular mechanics calculations. Alternatively, it could mean that the bound conformations are indeed substantially higher in energy than the global minimum. To distinguish these possibilities we have now undertaken full optimizations of bound conformations of methotrexate as well as the global minimum conformation and compared them with the energies of optimized and nonoptimized conformations derived from the 1.7-Å resolution data now available.[43] The results of these analyses, summarized in Table II, show that the energies of the conformations derived from the 2.5-Å data can be greatly reduced by geometry optimiza-

(41) Gund, P.; Poe, M.; Hoogsteen, K. H. *Mol. Pharmacol.* **1977**, *13*, 111.
(42) Matthews, D. A.; Alden, R. A.; Bolin, J. T.; Freer, S. T.; Hamlin, R.; Xuong, N.; Kraut, J.; Poe, M.; Williams, M.; Hoogsteen, K. *Science (Washington, D.C.)* **1977**, *197*, 452. Matthews, D. A.; Alden, R. A.; Bolin, J. T.; Filman, D. J.; Freer, S. T.; Hamlin, R.; Hol, W. G. J.; Kisliuk, R. L.; Pastore, E. J.; Plante, L. T.; Xuong, N.; Kraut, J. *J. Biol. Chem.* **1978**, *253*, 6946.
(43) Bolin, J. T.; Filman, D. J.; Matthews, D. A.; Hamlin, R. C.; Kraut, J. *J. Biol. Chem.* **1982** *257*, 13650.
(44) Spark, M. J.; Winkler, D. A.; Andrews, P. R. *Int. J. Quantum Chem., Quantum Biol. Symp.* **1982**, *9*, 321.

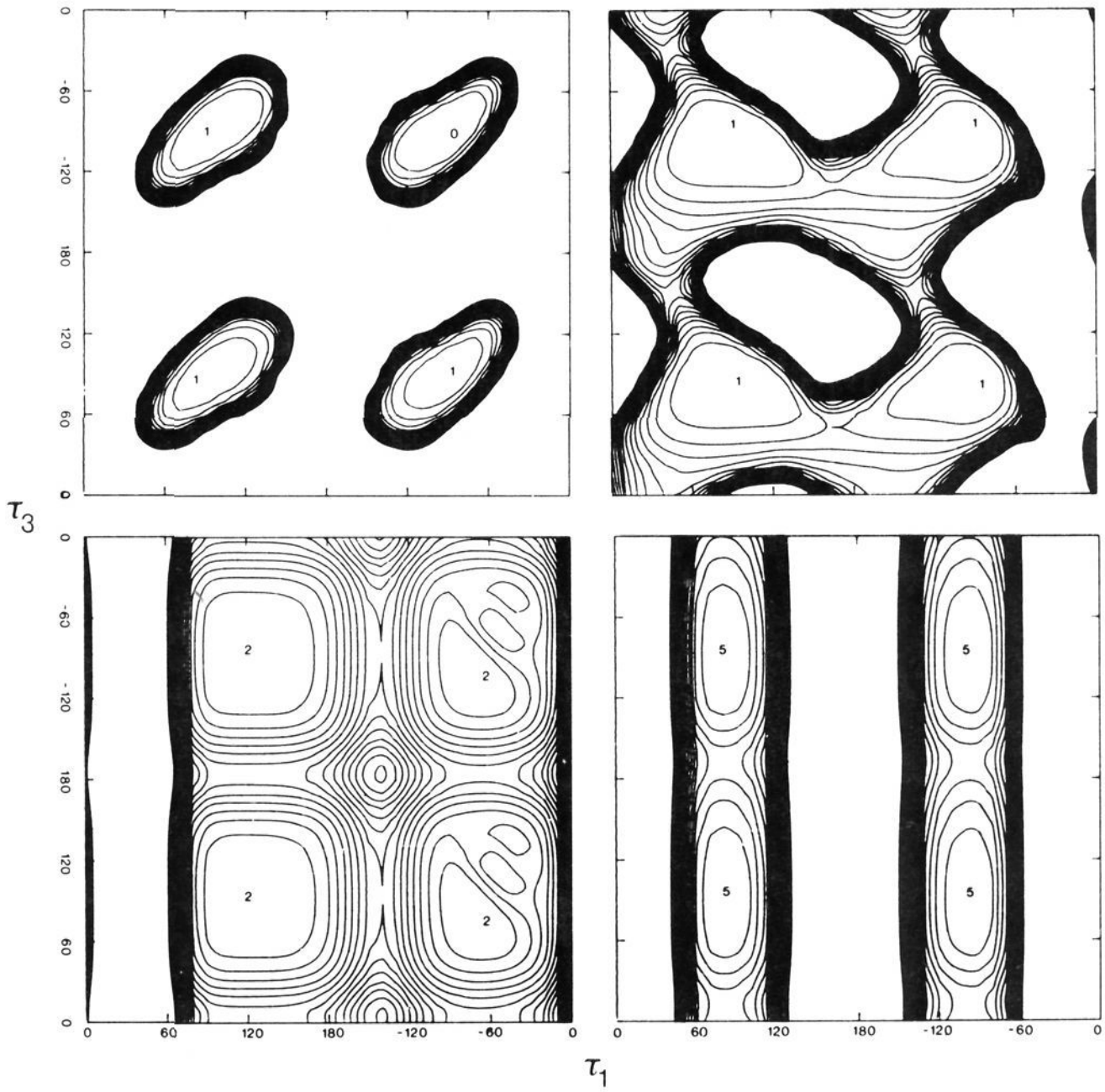

Figure 11. Contour maps describing relative energies for rotations τ_1 and τ_3 in **7** at various fixed values of τ_2: (a) $\tau_2 = 0°$; (b) $\tau_2 = 60°$; (c) $\tau_2 = 120°$; (d) $\tau_2 = 180°$. The first twenty 2.5 kcal/mol contour intervals are shown. Energies of minima are given in kilocalories/mole relative to the global minimum.

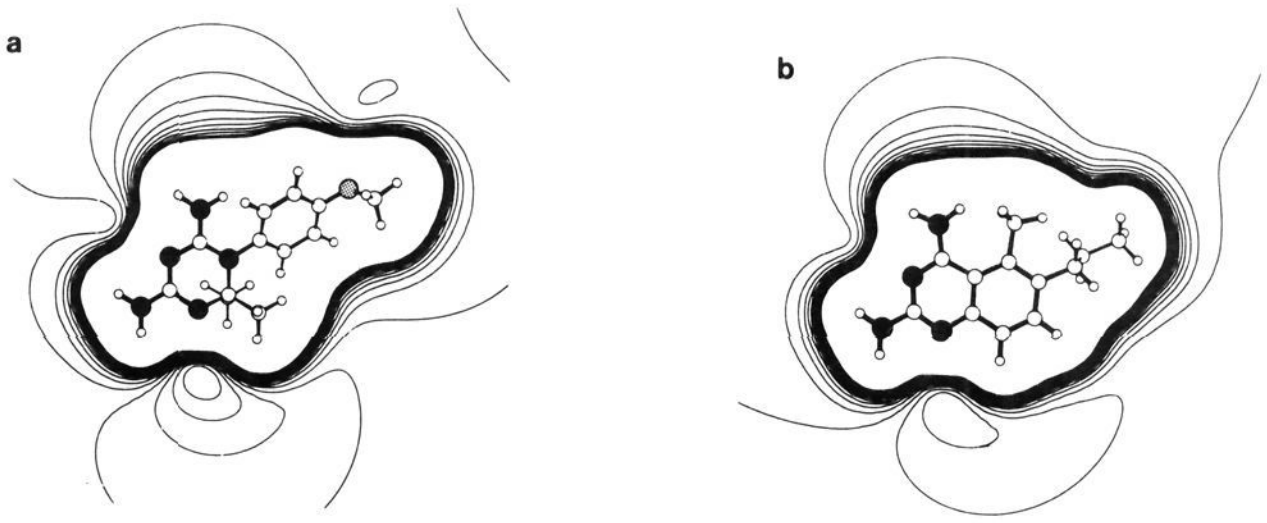

Figure 12. Electrostatic potential maps for some of the small molecule inhibitors of DHFR: (a) 2,4-diamino-6,6-dimethyl-5-(*p*-methoxyphenyl)-5,6-dihydrotriazine (**4**); (b) 2,4-diamino-5-methyl-6-propylquinazoline (**5**). In each case the potential surface shown is that in the plane of the heterocyclic ring. Fifteen 2 kcal/mol contour lines are shown.

tion without major changes in molecular conformation, but that these conformations nevertheless remain relatively high in energy (4–9 kcal/mol above the global minimum). However, the energies of both nonoptimized and optimized geometries obtained from the 1.7-Å data were still further reduced, with all three crystal conformations now falling within 3 kcal/mol of the global minimum. Thus, in contrast to our earlier finding,[44] the bound forms of methotrexate at both *E. coli* and *L. casei* DHFRs are in relatively low energy conformations.

Electrostatic Potentials. The net atomic charges on compounds **1**–**11** were determined in low-energy conformations by using CNDO/2. In all 11 molecules, partial charges of –0.2 to –0.4 are associated with N_1, N_2, and N_3, with corresponding positive charges on C_2 and C_4. In each of the inhibitors **1**–**8**, N_4 has a partial charge of ca. –0.25, somewhat less than that of ca. –0.4 on the corresponding atom (O_4) in the substrates **9**–**11**. These electronic characteristics of the heterocyclic rings are most clearly illustrated by the electrostatic potential maps given for representative examples of the small molecule inhibitors in Figure 12 and for the folates and folate analogues in Figure 13. These calculations have been performed on the nonprotonated ligands to indicate the likely sites for

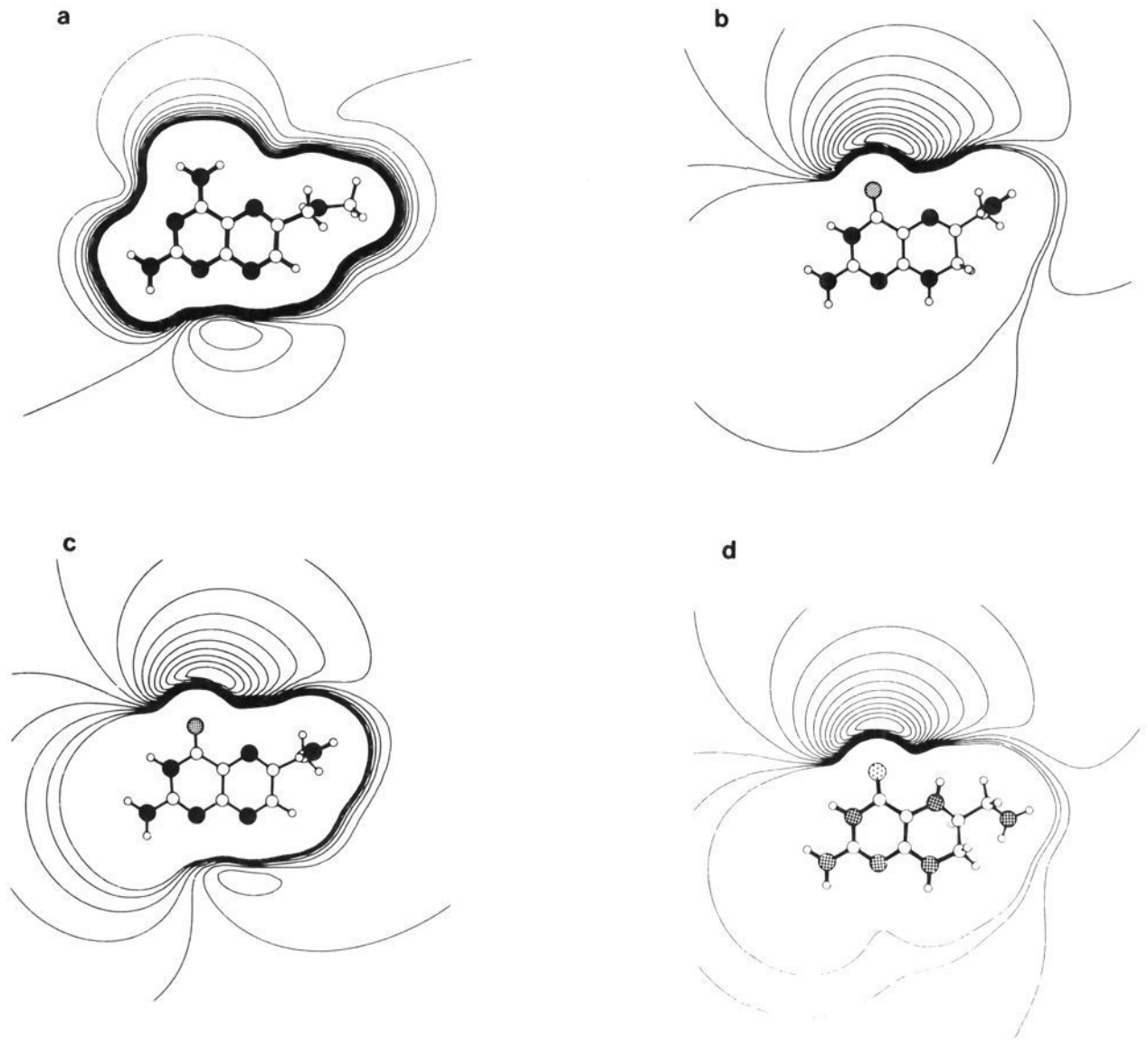

Figure 13. Electrostatic potential maps of (a) methotrexate (**7**), (b) dihydrofolate (**10**), (c) folate (**9**), (d) tetrahydrofolate (**11**). The global minima are −8, −26.7, −20.6, and −24.9 kcal/mol, respectively. For clarity, the benzoyl glutamate region has been removed from each structure.

protonation and thus the potential sites of strong interactions with the active site of the enzyme.

Each of the inhibitors has a negative potential well located near N_1 and a second, shallower minimum near N_3. The atom N_1 is known to be protonated when the pteridine ring of **7** interacts with an aspartate residue in the active site of DHFR, and the data suggest that all of the other inhibitors studied bind to the active site in the same way.

Of the substrate molecules, only folate has a potential energy well near N_1, and none has a minimum near N_3. However, all three folates **9**–**11** share a deep potential energy well associated with O_4.

Mode of Binding. Methotrexate (**7**) binds DHFR in the manner illustrated schematically in Figure 14a.[42,43] The most significant interaction is the ionic bond formed between the aspartate carboxyl ion of the enzyme and N_1 of **7**, which is thought to be protonated in the bound form.[21,23,45] This is entirely consistent with the calculated electrostatic potential surface (Figure 13a), which shows a large negative potential well between N_1 and N_8.

There is ample stereochemical and other evidence[42,45–47] to show that the pteridine ring of **10** is inverted relative to that of **7** when bound to the enzyme, although the benzoyl L-glutamate portions of both molecules appear to bind in the same way.[48,49] There is also evidence that suggests that **10** is in the nonprotonated 4-keto form when bound to the enzyme.[22] As noted previously,[44,50] these observations are in agreement with the calculated electrostatic potential for **10** (Figure 13b), which shows not only that the potential well associated with N_1 and N_8 in **7** is missing in **10** but also that a new potential minimum has appeared on the opposite edge of the pteridine ring, between O_4 and N_5.

Two alternative models have been proposed for the binding of **10** to DHFR. These are the direct inversion model (Figure 14b) suggested by Hitchings and Roth[51] and others[44,52] and the twisted inversion model (Figure 14c) proposed by Bolin et al.[43] Both models are reasonably consistent with the electrostatic potential data. In the direct inversion model the aspartate carboxyl group is presumed to be protonated, as suggested by kinetic evidence,[53] and it is this proton that would be most likely to occupy the potential energy well associated with O_4 and N_5. In the twisted inversion, the aspartate carboxyl is presumed to be anionic and interacts with the hydrogen associated with N_3 in the keto form of **10**. In both cases the interaction lacks the ionic component associated with the binding of **7**, which may explain the weaker binding between **10** and the enzyme.

(45) Gready, J. E. *Adv. Pharmacol. Chemother.* **1980**, *17*, 37.
(46) Fontecilla-Camps, J. C.; Bugg, C. E.; Temple, C.; Rose, J. D.; Montgomery, J. A.; Kisliuk, R. L. *J. Am. Chem. Soc.* **1979**, *101*, 6114.
(47) Charlton, P. A.; Young, D. W.; Birdsall, B.; Feeney, J.; Roberts, G. C. K. *J. Chem. Soc., Chem. Commun.* **1979**, 922.
(48) Pastore, E. J.; Plante, L. T.; Wright, J. M.; Kisliuk, R. L.; Kaplan, N. O. *Dev. Biochem.* **1979**, *4*, 477.
(49) Ozaki, Y.; King, R. W.; Carey, P. R. *Biochemistry* **1981**, *20*, 3219.
(50) Gund, P.; Andose, J. D.; Rhodes, J. B.; Smith, G. M. *Science (Washington, D.C.)* **1980**, *208*, 1425.
(51) Hitchings, G. H.; Roth, B. In "Enzyme Inhibitors as Drugs"; Sandler, M., Ed.; University Park Press: Baltimore, 1980; pp 263–280.
(52) Williams, J. W.; Morrison, J. F. *Biochemistry* **1981**, *20*, 6024.
(53) Stone, S. R.; Morrison, J. F. *Biochemistry* **1984**, *23*, 2753.

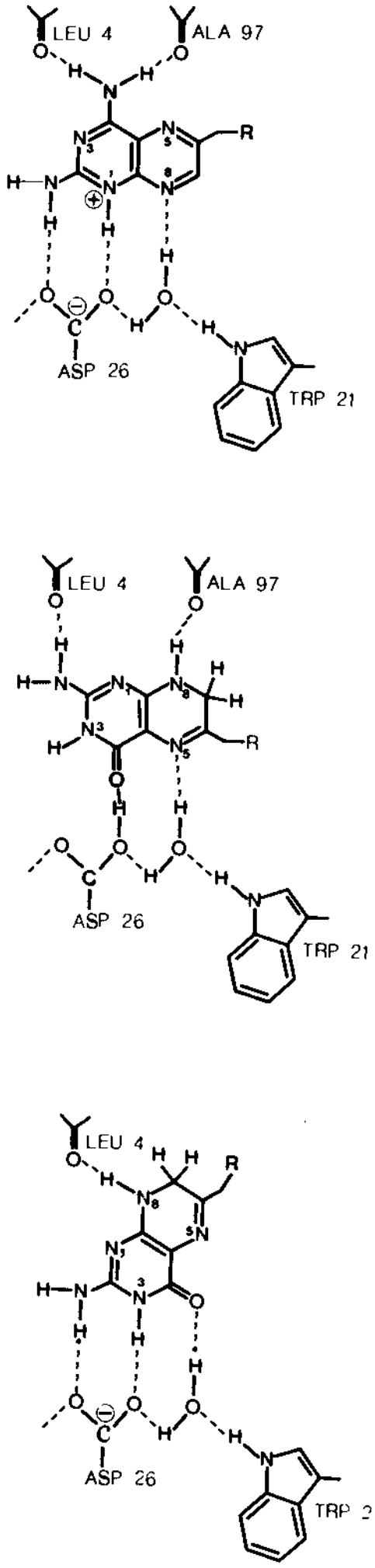

Figure 14. Schematic representation of binding of methotrexate (**7**) and dihydrofolate (**10**) to DHFR. Residues are numbered according to the sequence of the *L. casei* enzyme. (a) **7** in the orientation observed crystallographically;[41-43] (b) **10** in the inverted mode proposed by Hitchings and Roth[51] and other;[44,52] (c) **10** in the inverted binding mode proposed by Bolin et al.[43]

The direct inversion model has been rejected by Bolin et al.[43] on the grounds that they cannot construct a model that places N_5 of **10** near Asp-26 (of the *L. casei* enzyme) without a major change in protein conformation or violation of the assumption that the *p*-aminobenzoyl L-glutamate group is bound in the same manner as that of **7**. To check the latter point we have superimposed **10** onto each of three conformations of **7** observed in its complexes

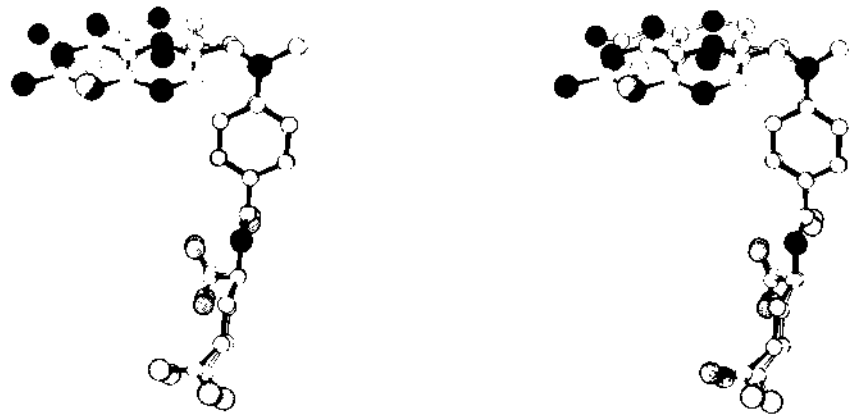

Figure 15. Stereoscopic view of the superimposition of **10** on **7** (solid bonds) according to the direct inversion model. The conformation of **7** is that observed in the crystal structure of its ternary complex with *L. casei* DHFR and NADPH.[42]

with DHFR. This was done initially for the 2.5-Å data and later verified at 1.7 Å. Figure 15 is a stereoscopic view of the result of this superimposition onto the conformation of **7** bound to the enzyme from *L. casei*, and equally good agreement is obtained for the two *E. coli* conformations. In each case, the nonoptimized energies of the matching conformations are lower than those of **7** itself, and full geometry optimization with MM2 brought all three structures to less than 2 kcal/mol above the global minimum. The fit of these conformations to DHFR is less satisfactory because of a close contact (1.7 Å) between the N_2 amino group of **10** and the side chain of Leu-4 of the enzyme. It is clear, however, that this interaction could be alleviated by a relatively slight movement of either the Leu-4 residue or the substrate. In the latter case the proton associated with the aspartate carboxyl group would move from the center of the electrostatic minimum near O_4 to a position at the N_3 end of the same potential energy well. Transfer of this proton to N_5 could then occur either via an intermediate water molecule or by direct movement of the proton to the other side of O_4. The latter mechanism is favored by the electrostatic potential map (Figure 13b), which shows a single continuous minimum from O_4 to N_5. Such a movement of the proton would alter the interaction from an essentially nonionic one to an almost completely ionic bond, thus greatly enhancing the binding of the transition state of the reaction. The direct inversion model is thus significantly favored by this explanation for the transfer of a proton to N_5, for which there is no obvious mechanism in the twisted inversion model.[43]

Unlike dihydrofolate, the electrostatic potential map for folate (Figure 13c) shows minima on both edges of the pteridine ring, suggesting that folate could bind in either the same way or inverted with respect to methotrexate. Superimposition and energy calculations corresponding to those for **10** above show that conformations of both types are energetically accessible after superimposition onto **7** in any of its bound conformations, with the inverted conformations being slightly lower in energy. These data suggest that folate could act either as a substrate, by binding in an inverted conformation,[47] or as an inhibitor, by binding in the same way as methotrexate. In the substrate case, folate could interact with the enzyme in either of the inverted models proposed above, although proton transfer to N_8 clearly cannot be from Asp-26. Bolin et al.[43] suggest the carbonyl oxygen of Leu-4, Ala-97, or both as a possible source of this proton, presumably by transfer from an associated water molecule. A similar mechanism could be proposed for the direct inversion model. In either case, the relative slowness of folate catalysis would be explained by less efficient proton transfer via the carbonyl oxygens as well as a less satisfactory orientation for hydride transfer from NADPH.

Another factor that may be important in considering the relative merits of the direct inversion and twisted inversion models for substrate binding is the considerable conformational flexibility of the connecting chain revealed by the present calculations. The flexibility around τ_2, in particular, and to a lesser extent τ_1, means that the pteridine ring can actually swivel *between* the models of Figures 14b and 14c without encountering any significant energy barrier and with minimal disturbance of the benzoyl L-glutamate anchoring group. Although these observations are based on calculations for the isolated ligand, computer graphics modelling suggests that there is sufficient space in the active site to allow this conformational change to occur in the bound ligand. It should thus be possible, for example, for folate to bind as a substrate in the manner shown in Figure 14c but, after conversion to **10** by protonation at N_8 and hydride transfer to C_7, to twist into conformation **14b** for subsequent reduction to tetrahydrofolate. The electrostatic potential calculations show that in the absence of further protonation one would expect a net repulsive interaction between Asp-26 and **11**, which should lead to the rapid expulsion of **11** from the active site.

Species Specificity. The selectivity of DHFR inhibitors for the enzyme from different species is well known,[1,54] with methotrexate being relatively nonselective, the phenyldihydrotriazines favoring mammalian enzymes, trimethoprim selectively inhibiting enzymes from bacteria, and pyrimethamine being moderately selective for protozoal DHFR. These differences in selectivity are presumably due to differences in the electronic or steric character of the inhibitors. Since the electrostatic potentials show that all of the inhibitors studied are capable of forming similar interactions between their heterocyclic rings and the active site, this suggests that conformational differences may be of major importance in determining selectivity. To test this possibility we have chosen one of the present series of inhibitors as a model compound for binding to each of the three classes of DHFR listed above. The remainder of the inhibitors have then been superimposed onto the likely active conformations of the model inhibitors by using the electrostatic potentials as a guide and allowing their conformations to vary over the full range of calculated low-energy forms to give the best fit to the model compounds.

In the absence of a published crystal structure for a mammalian DHFR, the conformation of dihydrotriazine **4** bound to avian DHFR[37] was chosen to model inhibition of eukaryotic enzymes. QSAR studies[55] have shown that dihydrotriazine binding requirements are similar, although not identical, for a number of eukaryotic DHFRs. All of the inhibitors matched **4** reasonably well in low-energy conformations, although in some cases the conformations favored on the basis of the superimpositions were found to be poor fits to the active site. Trimethoprim (**1**) in particular superimposes nicely on **4** with the heterocyclic rings, aromatic rings, and one methoxy group of the two inhibitors all being well matched (Figure 16). Despite the quality of this fit, however, and the fact that this conformation of **1** appears to fit reasonably well into the active site, X-ray diffraction data[34] show that the actual binding mode of **1** to chicken liver DHFR is significantly different to that suggested by Figure 16. Indeed, the phenyl ring

Figure 16. Stereoscopic view of **1** superimposed on the conformation of **4** observed in its crystalline complex with chicken liver DHFR.[37] Note that in this illustration the 1- and 3-methoxy groups are in nonplanar conformations which, according to the nonbonded energy calculations, are marginally preferred to the planar ones.

of **1** in the bound conformation is rotated through ca. 90° (τ_2) relative to that shown, with the result that there is a substantial displacement of an active-site tyrosine in the ternary complex. Matthews et al.[34] suggest four possible explanations for the failure of **1** to bind tightly to the avian enzyme. These are (1) differences in the geometries of the hydrophobic pockets in avian and bacterial DHFRs, (2) inability to form a hydrogen bond to the 4-amino group in the avian enzyme, (3) movement of the tyrosine-31 residue, and (4) energy differences between conformations providing optimal matches to the two sites. The present calculations (Figures 2 and 16) show that conformations matching both sites are low in energy (less than 1 kcal/mol), and Matthews et al.[34] have produced arguments to show that the tyrosine movement requires minimal energy. It thus appears that, contrary to the superficial impression given by Figure 16, trimethoprim cannot fit the dihydrotriazine-binding hydrophobic pocket of the avian enzyme without partially destroying its interaction with the 2,4-diamino heterocycle. The fact that other inhibitors, notably **2** and **3**, appear to provide a good match for the bound conformation of **4**, as well as a reasonable fit to the active site, is thus not sufficient to guarantee inhibitory activity against this enzyme.

The crystal structure of **1** bound to *E. coli* DHFR[56] was used as the model for inhibition of bacterial DHFR. Apart from **7**, which provides a reasonable match to **1** in several low-energy conformations as well as that observed in the bound complex,[42,57] none of the inhibitors provided a satisfactory superimposition of both heterocyclic rings and aromatic rings simultaneously. This is consistent with the relative lack of potent antibacterial activity in the other inhibitors.

Since no crystal structures for protozoal DHFRs are available, the lowest energy conformation of the antimalarial **2** was used to model this class. All of the inhibitors studied provided a reasonable match to this conformation of **2**, which is not dissimilar to that observed for the dihydrotriazine **4** bound to chicken liver DHFR. Thus, although these superimpositions are consistent with inhibition of protozoal DHFR by all of the present inhibitors tested, the quality of the fit alone is not sufficient to suggest antimalarial activity in the other inhibitors.

None of the preceding superimpositions fully define the likely side-chain orientation of the larger inhibitors, **5–7**, each of which seems likely to bind in a similar conformation. Indeed, using the conformation of **7** observed[42] in its crystal complex with *L. casei* as a guide, both **5** and **6** were found to fit **7** well in reasonably low-energy conformations. The superimpositions favored *cis*-**6** over the

(54) Beddell, C. R. In "X-Ray Crystallography and Drug Action"; Horn, A. S., De Ranter, C. J., Eds.; Clarendon Press: Oxford, 1984; Chapter 10.
(55) Blaney, J. M.; Hansch, C.; Silipo, C.; Vittoria, A. *Chem. Rev.* 1984, *84*, 333.
(56) Baker, D. J.; Beddell, C. R.; Champness, J. N.; Goodford, P. J.; Norrington, D. R.; Smith, D. R.; Stammers, D. K. *FEBS Lett.* 1981, *126*, 49.
(57) Matthews, D. A.; Bolin, J. T.; Burridge, J. M.; Filman, D. J.; Volz, K. W.; Kaufman, B. T.; Beddell, C. R.; Champness, J. N.; Stammers, D. K.; Kraut, J. *J. Biol. Chem.* 1985, *260*, 381.

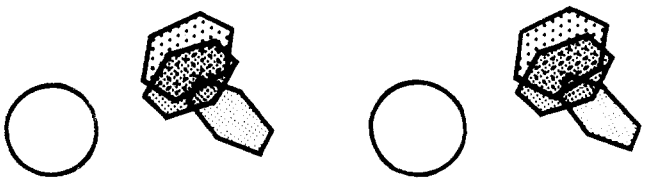

Figure 17. Schematic and stereoscopic view of the three specific model compounds in their most likely biologically active conformations and with their $N_1C_2N_3C_4$ regions (circle) superimposed. The aromatic groups are those for malarial (top), mammalian (center), and bacterial (bottom) enzyme inhibitors.

slightly higher energy trans isomer, although fitting both structures to the active site gave a somewhat better fit for the trans form. The cis form is also favored by Hopfinger and co-workers[58] on the basis of their calculated potential energies and molecular shape analysis. As noted above, the fit of **1** to **7** is also quite satisfactory, with a good superimposition of the two molecules in their enzyme-bound conformations.[57] Kuyper et al.[59,60] have taken advantage of this fact by replacing the 3′-OCH_3 of **1** with an extended chain ending with a carboxyl group capable of interacting specifically with the α-carboxyl binding site. A similar increase in inhibitory activity has been obtained by analogous modification of brodimoprim.[61,62]

The three specific model inhibitors are illustrated in Figure 17, where the heterocycle is shown as a common binding region (circle), but the hydrophobic binding region is slightly different in each model. There is significant overlap between the mammalian and protozoal hydrophobic binding regions but not with the bacterial. This could account for the similar activities of many DHFR inhibitors against both mammalian and protozoal DHFRs and the great difference in inhibition of bacterial and mammalian enzymes.

Conclusions

Over the past few years, so much information has accumulated relating to DHFRs and their inhibitors that the enzyme has now virtually acquired the status of a laboratory in which new ideas and techniques related to inhibitor design can be implemented and tested. It was therefore of interest to apply the conformational energy calculations and modelling methods that we have used for other systems to the substrates and inhibitors of DHFR.

Although the molecules studied here are too large and flexible to allow complete potential energy surface calculations including full geometry optimization, the approximate calculations reported provide a reasonable method for qualitatively determining all the conformations accessible to the molecules. In this context it is noteworthy that geometry optimization could only increase the total number of low-energy conformations obtained. Despite this limitation, virtually all the compounds studied have a large number of readily accessible conformations. Where crystal structures are available for the free inhibitors, they fall in or near one of these calculated low-energy regions. This applies to both free and enzyme-bound forms. However, any one of the low-energy conformations is a potentially biologically active form, and there is no way of distinguishing, using calculations alone, which conformations are responsible for activity.

The calculated electrostatic potentials are in good agreement with available experimental data on sites of protonation, etc., and illustrate important common features of the inhibitors that also appear to be relevant to binding. The differences in electrostatic potentials between the inhibitors and the substrates alone provide a simple explanation for the inverted binding mode of the substrates relative to the inhibitors, and the combination of these data with the energy calculations provides a fully consistent explanation for these observations. It is also clear that the combination of the electrostatic potential and the energy data could have been used in advance to predict this inverted binding mode, even if the biochemical data had not already suggested it. The inverted binding mode *could* thus have been predicted on the basis of the calculations alone; whether, in the absence of the experimental observation, we *would* have predicted it, is another question.

Similar questions arise from the use of the calculated energies and electrostatic potentials to explain the selectivity data. The conclusions of this part of the work are summarized by the relatively slight variation in aromatic ring placement illustrated for the various classes in Figure 17. These findings are confirmed, at least for the bacterial and avian enzymes, by the finding of Matthews et al.[34,57] that the hydrophobic binding clefts occupied by tight-binding inhibitors of the two enzymes are in quite different orientations relative to the 2,4-diamino heterocycles. However, although these differences can be used to explain the selectivity of each of the inhibitors included in the analysis, the spatial distinctions indicated in Figure 17 are not clear enough to suggest the possibility of predicting the selectivities of as yet untested compounds. The excellent but irrelevant match of inhibitors **1** and **4** is perhaps the strongest evidence on this point. On the other hand, there is no doubt that data of this type can provide positive guidance in the development of new compounds. The design of methotrexate-like trimethoprim and brodimoprim analogues[59-62] is an excellent example.

Registry No. **1**, 738-70-5; **2**, 58-14-0; **3**, 100811-99-2; **4**, 21316-30-3; **5**, 67697-09-0; **6**, 55096-47-4; **7**, 59-05-2; **8**, 54-62-6; **9**, 59-30-3; **10**, 4033-27-6; **11**, 135-16-0; DHFR, 9002-03-3.

(58) Battershell, C.; Malhotra, D.; Hopfinger, A. J. *J. Med. Chem.* **1981**, *24*, 812.
(59) Kuyper, L. F.; Roth, B.; Baccanari, D. P.; Ferone, R.; Beddell, C. R.; Champness, J. N.; Stammers, D. K.; Dann, J. G.; Norrington, F. E.; Baker, D. J.; Goodford, P. J. *J. Med. Chem.* **1982**, *25*, 1120.
(60) Kuyper, L. F.; Roth, B.; Baccanari, D. P.; Ferone, R.; Beddell, C. R.; Champness, J. N.; Stammers, D. K.; Dann, J. G.; Norrington, F. E.; Baker, D. J.; Goodford, P. J. *J. Med. Chem.* **1985**, *28*, 303.
(61) Kompis, I.; Then, R. L. *Eur. J. Med. Chem.* **1984**, *19*, 529.
(62) Birdsall, B.; Feeney, J.; Pascual, C.; Roberts, G. C. K.; Kompis, I.; Then, R. L.; Muller, K.; Kroehn, A. *J. Med. Chem.* **1984**, *27*, 1672.